

A Resistive Linear Antenna for Ground-Penetrating Radars

Kangwook Kim and Waymond R. Scott, Jr.

School of Electrical and Computer Engineering
Georgia Institute of Technology
Atlanta, Georgia 30332-0250

ABSTRACT

The resistive vee dipole (RVD) loaded with the Wu-King profile has many advantages for use in ground-penetrating radar (GPR) applications. It can be designed to transmit a temporally-short pulse to a small spot on the ground. The shape of the transmitted pulse is simply related to the input signal, e.g., a derivative. The RVD also has a low radar cross section. In addition, it can be easily manufactured using a circuit board and discretely loading it with chip resistors. One drawback of the RVD is that the input impedance of the RVD increases significantly with decreasing frequency and, therefore, has a high voltage standing wave ratio (VSWR) at low frequencies, which limits the low-frequency response of the antenna. To improve the low-frequency response, a discretely-loaded resistive linear antenna (RLA) has been developed, whose basic principle of operation is the same as that of the RVD. The RLA has curved arms loaded with a modified Wu-King profile instead of straight arms loaded with the Wu-King profile. With an appropriate selection of the curve and the loading profile, the low-frequency response is significantly better for the RLA than for the RVD. The RLA has been developed using a method of moments code. The performance of the RLA is validated both numerically and experimentally.

Keywords: Loaded antenna, resistive vee dipole (RVD), ground-penetrating radar (GPR)

1. INTRODUCTION

A resistively-loaded vee dipole (RVD) is a vee dipole with each arm loaded with a resistive profile.¹⁻³ In a short-pulse ground-penetrating radar (GPR) application, the Wu-King profile is usually chosen for the resistive profile because an RVD with the Wu-King profile can be made to radiate a short pulse into a small spot on the ground while having a low radar cross section.⁴⁻⁸ In addition, it is geometrically simple and light; thus, it can be easily applied to an array application for a hand-held system with a small number of elements or for a vehicle-mounted system with a large number of elements.⁹

However, the RVD has several drawbacks. First, the input impedance of the RVD increases significantly with decreasing frequency and, therefore, has a high voltage standing wave ratio (VSWR) at low frequencies. This limits the low frequency response of the antenna. Another drawback is that it is difficult to build an RVD with a continuous resistive profile while being mechanically strong. We have previously developed a way to build a mechanically-strong RVD with an accurate resistive profile and demonstrated its performance.⁹ In the previous work, the antenna arms were printed on a thin Kapton film and surface-mount chip resistors were loaded such that they approximate the continuous resistive profile. The antenna was then attached to a thick FR-4 frame to enhance the mechanical strength. While this antenna had an accurate resistive profile, the structure needed improvement because delicate components such as chip resistors were exposed.

In this paper, we present a resistive linear antenna (RLA), which is an improved version of the RVD. To improve the VSWR, we used curved arms instead of straight arms and loaded the arms with a modified Wu-King resistive profile. This also improves other characteristics, such as the gain and front-to-back ratio. The mechanical reliability is improved by inserting the antenna between two blocks of polystyrene foam instead of attaching it to an FR-4 frame. The resulting structure is more robust and easier to handle because all the delicate components are covered by the polystyrene foam.

Further author information: (Send correspondence to K. Kim)

K. Kim: E-mail: kangwook.kim@ece.gatech.edu, Telephone: 1 404 894 3123

W. R. Scott: E-mail: waymond.scott@ece.gatech.edu, Telephone: 1 404 894 3048

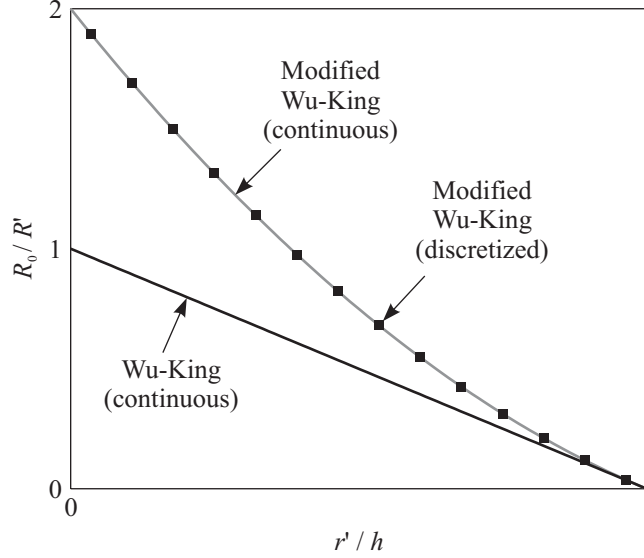


Figure 1. Resistive loading profiles of the continuous Wu-King, continuous modified Wu-King, and discrete modified Wu-King in terms of conductivity.

2. ANTENNA DESIGN

The Wu-King resistive profile (R') can be written as the resistance per unit length as:

$$R'(r') = \frac{R_0}{1 - (r'/h)}, \quad (1)$$

where r' is the distance along the arm from the drive point, h is the length of the arm, and R_0 is the resistance per unit length at the drive point. With an appropriate selection of R_0 , a current pulse injected into the RVD travels with a negligible internal reflection. However, a current pulse incident in the feed line is significantly reflected by the Wu-King profile at the drive point because the resistance per unit length jumps from zero in the feed line to $R' = R_0$ at the drive point ($r' = 0$). This reflection can be lowered by selecting a lower R_0 than the appropriate value. However, this will lower the resistive profile throughout the entire arm, which increases reflection at the open end of the antenna.

In order to lower R' at the drive point while maintaining small open-end reflection, the Wu-King profile is modified to

$$R'_m(r') = \left\{ \frac{1 - (r'/h)}{R_0} + \frac{[1 - (r'/h)]^2}{R_{0m}} \right\}^{-1}, \quad (2)$$

where R_{0m} is a parameter that modifies the resistive profile. This equation is equivalent to Eq. (1) when $R_{0m} = \infty$. In Eq. (2), R'_m at the drive point decreases with decreasing R_{0m} , while R'_m at the antenna open end always converges to $R'(r' = h)$. In this work, we choose $R_{0m}/R_0 = 1.0$. The modified Wu-King profile with $R_{0m}/R_0 = 1.0$ is compared with the original Wu-King profile in Fig. 1. The figure shows that the resistance per unit length of the modified Wu-King profile at the drive point is reduced to half of that of the original Wu-King profile ($R'_m(0) = 0.5R'(0)$). Both profiles converge to infinity at the antenna open end.

Another reason for currents to be reflected at the drive point is that the geometry changes abruptly from a feed line to the antenna. Thus, the reflection can be reduced by smoothly changing the antenna shape from the feed line. In this work, the shape of the RLA varies according to the following equations:

$$y = \begin{cases} y_1 = ae^{bz}, & 0 \leq z < z_0, \\ y_2 = c_0 + c_1(z - z_0) + c_2(z - z_0)^2, & z_0 \leq z \leq L. \end{cases} \quad (3)$$

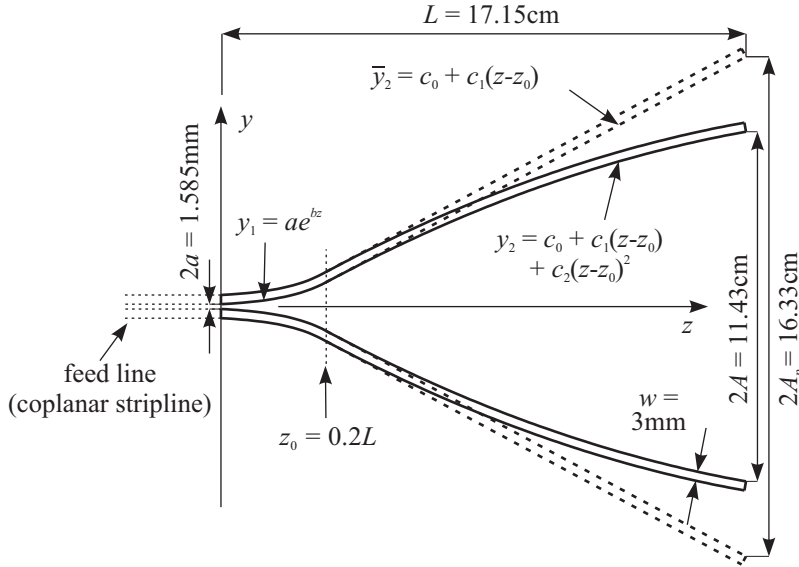


Figure 2. Description of the antenna shape. The solid lines show the designed antenna shape. The dotted lines on the right-hand side show the shape of the antenna if the curve were straight over the interval $z_0 \leq z \leq L$.

Fig. 2 shows the diagram of the antenna generated from these equations. The curve grows exponentially over the interval $0 < z \leq z_0$ and grows at a slower rate over the interval $z_0 \leq z \leq L$, where L is the length of the antenna in the z -direction. The antenna is fed by a coplanar stripline with the characteristic impedance Z_0 . The parameter a is determined such that the drive point of the antenna has the same characteristic impedance as the feed line, when the antenna resistive loading is ignored. The parameters b , c_0 , c_1 , and c_2 are determined according to the following relations:

$$\begin{aligned}
 ae^{bz_0} &= c_0, & y_1 &= y_2 \text{ at } z = z_0, \\
 abe^{bz_0} &= c_1, & y_1' &= y_2' \text{ at } z = z_0, \\
 c_0 + c_1(L - z_0) &= A_p, & \bar{y}_2 &= A_p \text{ at } z = L, \\
 c_0 + c_1(L - z_0) + c_2(L - z_0)^2 &= A, & y_2 &= A \text{ at } z = L,
 \end{aligned} \tag{4}$$

where A_p is a half of the aperture size if the curve were straight over the interval $z_0 \leq z \leq L$, and A is a half of the aperture size. In this work, the chosen parameters are $Z_0 = 200\Omega$, $2A = 11.43\text{cm}$, $2A_p = 16.33\text{cm}$, $L = 17.15\text{cm}$, and $z_0/L = 0.2$. The width of the stripline is chosen to be 3mm. Thus, the coplanar stripline geometry at the drive point requires $2a = 1.585\text{mm}$ to have $Z_0 = 200\Omega$.¹⁰ The parameters determined from Eqs. (3) and (4) are $b = 67.34$, $c_0 = 0.007976$, $c_1 = 0.5371$, and $c_2 = -1.302$.

3. NUMERICAL ANALYSIS

Three antennas are numerically analyzed using EIGER, a method of moments code.¹¹ The antennas are an RVD with straight arms and continuous Wu-King profile, the RLA with curved arms and continuous modified Wu-King profile, and the RLA with curved arms and discrete modified Wu-King profile. The common parameters for the antennas are length $L = 17.15\text{cm}$, aperture size $2A = 11.43\text{cm}$, width of striplines $w = 3\text{mm}$, and resistance per unit length normalized by the arm length $R_0h = 467.1\Omega$. For the RLA with discrete profile, the continuous profile is discretized by 14 resistors, whose values are marked by rectangles in Fig. 1. The resistors are modeled by a patch with an appropriate surface resistance; the width and length of each patch are 1.25mm and 1.2mm, respectively. In this section, the antennas are fed by a 200 Ω transmission line.

Fig. 3 shows the VSWR's of the antennas. The VSWR of the RLA is significantly lowered at low frequencies, essentially extending the lower end of the bandwidth. The bandwidth with VSWR = 2.0 begins at 1.19GHz

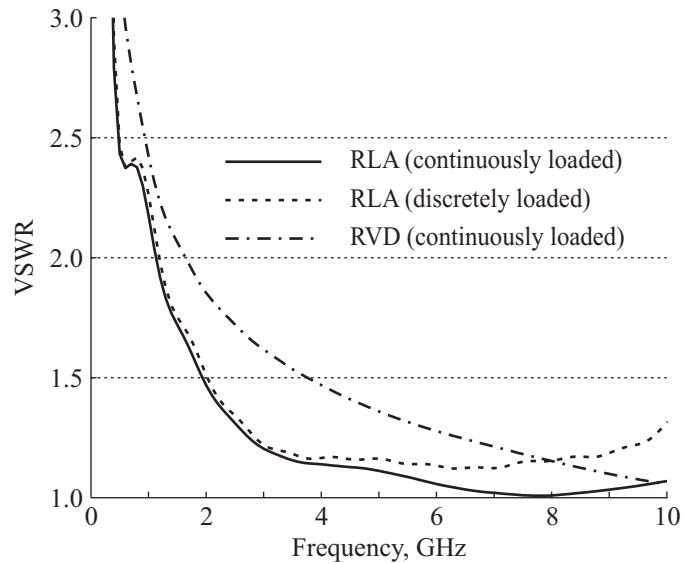


Figure 3. Voltage standing wave ratios of the continuously loaded RVD, continuously loaded RLA, and discretely loaded RLA as functions of frequency.

for the RLA with discretized loading and 1.64GHz for the RVD with continuous loading. The bandwidth with $VSWR = 1.5$ begins at 2.23GHz for the RLA with discretized loading and 3.76GHz for the RVD with continuous loading. Note that the VSWR for the RLA with discretized profile is slightly worse than the other antennas for frequencies higher than 8GHz. The reason for this is the resonant frequency of the resistor spacing. The length of the antenna arm along the curve is 19.1cm. With 14 resistors, the average resistor spacing is 1.36cm. The first resonant frequency of this spacing is approximately 11GHz. The effect of the resonant behavior begins to appear at 10GHz in the figure. This behavior gives a rough guideline on how many resistors need to be used. Clearly, the more number of resistors need to be used if one wants a broader bandwidth.

Fig. 4 shows the gains of the antennas as functions of frequency. Here, the gain is defined as

$$\text{gain} = 4\pi \frac{\text{radiation intensity}}{\text{power incident in the feed line}}. \quad (5)$$

The figure shows that the RLA's have higher gains than the RVD. The discretization of the loading profile does not seem to affect the gain much for frequencies less than 8GHz. The gain of the RLA is deteriorated by the discretization at frequencies higher than 8GHz. Note that the gains are relatively low for all the three antennas. The reason for this is that a large portion of the incident energy is dissipated in the resistors as well as reflected at the drive point.^{5,12} Thus, the radiation efficiencies of the antennas are low.

The low radiation efficiency of the antenna is not a problem for a GPR because of the close proximity to the targets. The reflections from the equipment behind the antenna and the multiple reflections between the antenna and the surface of the ground are bigger issues. The rejection of the signals from behind an antenna, such as the reflected signal from the equipment, can be measured by the front-to-back ratio (F/B). Fig. 5 shows the F/B's of the antennas in a dB-scale. The F/B of the RLA is higher for most frequencies than that of the RVD. The improvement is significant around 2GHz for both continuously and discretely loaded RLA's. The improvement at 2GHz may be particularly useful because the GPR in this work depends much on the frequency content around this frequency.

The multiple reflections between the antenna and the surface of the ground can be lowered by designing the antenna to be less reflective, e.g., to have low RCS at the boresight angle. Fig. 6 shows the monostatic RCS observed at the boresight of the antenna. The RCS is improved at most frequencies with use of the curved arms and continuous modified Wu-King profile. However, the RCS is deteriorated by the discretization of the

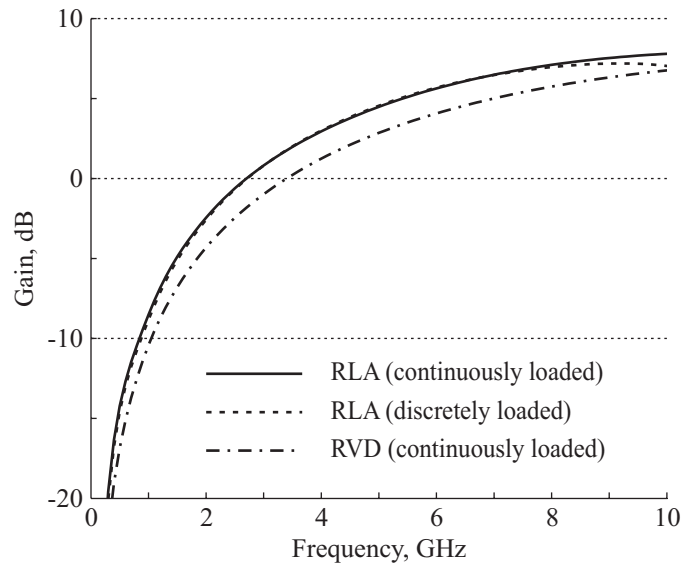


Figure 4. Gains of the continuously loaded RVD, continuously loaded RLA, and discretely loaded RLA in dB.

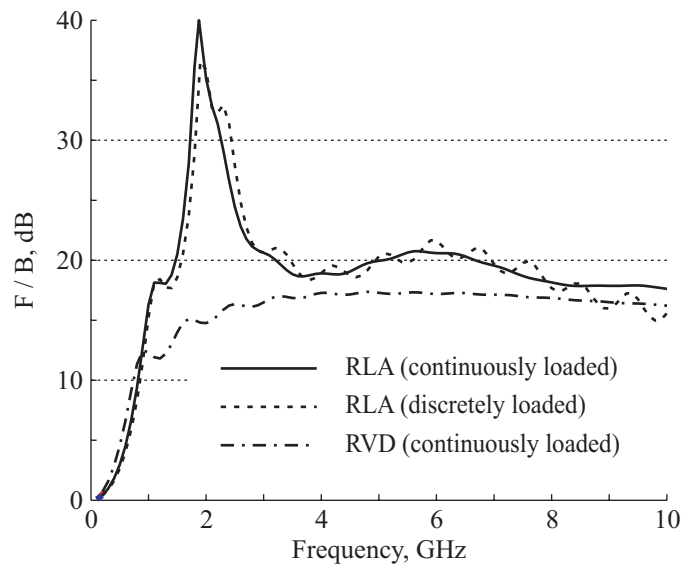


Figure 5. Front-to-back ratios of the continuously loaded RVD, continuously loaded RLA, and discretely loaded RLA in dB.

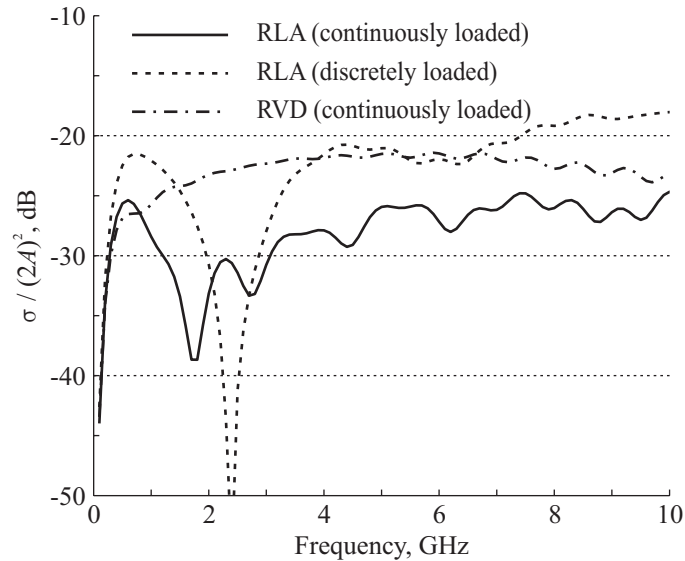


Figure 6. Radar cross sections of the continuously loaded RVD, continuously loaded RLA, and discretely loaded RLA in dB. The RCS's are normalized by the aperture length squared.

continuous profile. Note that the RCS for the discretely loaded RLA is still comparable to the RCS for the RVD over the frequency range $1.5\text{GHz} < f < 7\text{GHz}$.

Finally, Fig. 7 shows the gain patterns of the antennas in the E - and H -planes at eight frequency points. Each curve is normalized by its maximum and drawn on a 30dB-scale. Fig. 7 (c) shows that the backward radiation of the RLA is negligible at $f = 2\text{GHz}$, which is also shown in Fig. 5. In Figs. 7 (d) – (h), back lobes are seen for the RLA's; however, their normalized amplitudes are smaller than backward radiation of the RVD. Note that in Figs. 7 (d) – (h), nulls are seen around 90° both in the E - and H -planes. This may result in less coupling between adjacent elements in an array.

4. ANTENNA MEASUREMENT

The RLA with discretized loading profile has been manufactured. The antenna arms are printed on a $50.8\mu\text{m}$ -thick (2mil) Kapton substrate. Each arm is loaded with 14 surface-mount chip resistors, whose width and length are 1.25mm and 2.0mm, respectively*. The resistors approximate the continuous profile over the operating frequency band. The antenna is fed by a double-Y balun/transformer, whose characteristic impedance at the antenna drive point is approximately 188Ω .¹³ Note that the antenna structure made in this method is very fragile. In the previous work, we attached the antenna structure to a thick FR-4 frame to enhance the mechanical strength.⁹ The resulting structure was strong enough to be used in the experiment with care. However, it may not be usable in the field because the resistors are exposed and prone to damage. Thus, in this work, we increased the mechanical reliability of the antenna by squeezing it between two 2.54cm-thick polystyrene foam blocks. Fig. 8 shows the implemented antenna structure. Because all the delicate parts are shielded by the polystyrene foam blocks, this structure may be used in the field.

The performance of the manufactured antenna is measured in terms of VSWR and gain. The measurement is compared with the numerical results. Fig. 9 shows the VSWR of the RLA when the RLA is connected to a 188Ω feed line, which is the output characteristic impedance of the double-Y balun used in this work. The graph shows that the manufactured RLA works very well. Fig. 10 shows the gain of the antenna module (RLA and balun). For the gain measurement, two identically-manufactured antennas are used. The antennas are separated by a distance R and pointed at each other. Then, the transmission coefficient (S_{21}) is measured at each frequency.

*The resistors are terminated with 0.4mm-long metal leads at both ends. Thus, the effective length of the resistive film is 1.2mm, which is the dimension used for the length of the resistive patch in the numerical model.

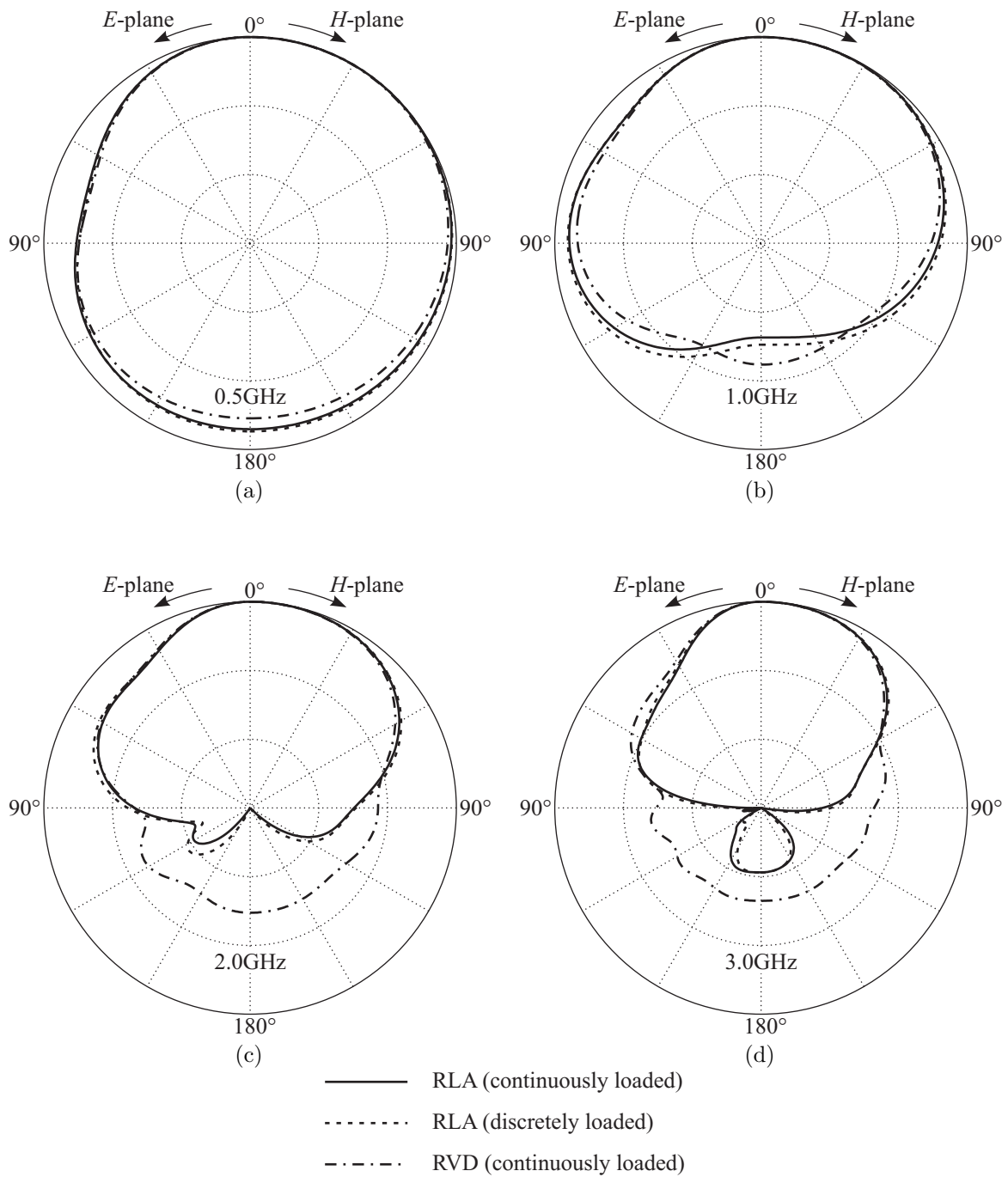


Figure 7. Normalized gain patterns of the continuously loaded RVD, continuously loaded RLA, and discretely loaded RLA in a 30-dB scale. The left- and right-hand sides of each graph are the gain patterns observed in the principal *E*- and *H*-planes, respectively.

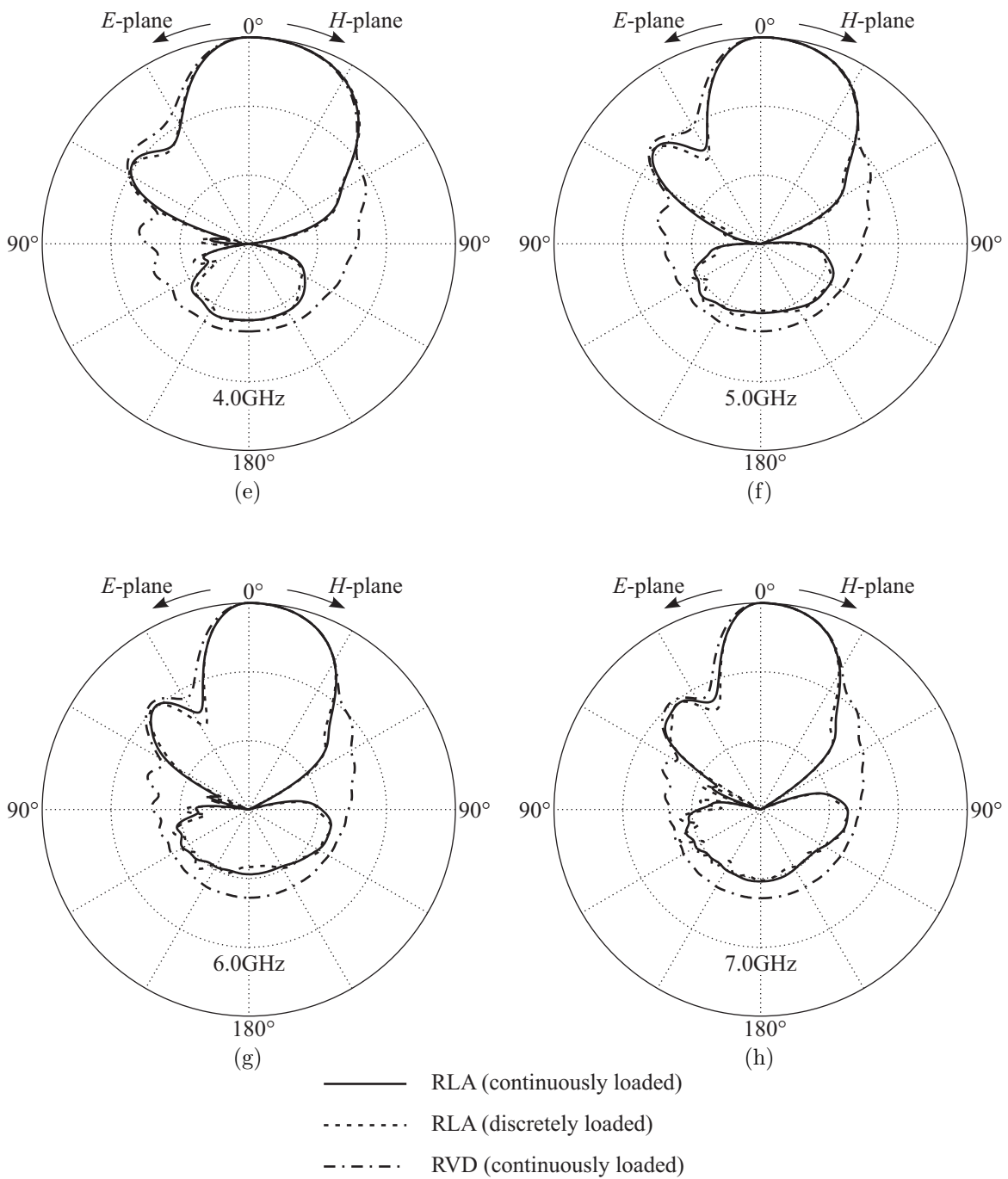


Figure 7. Continued.

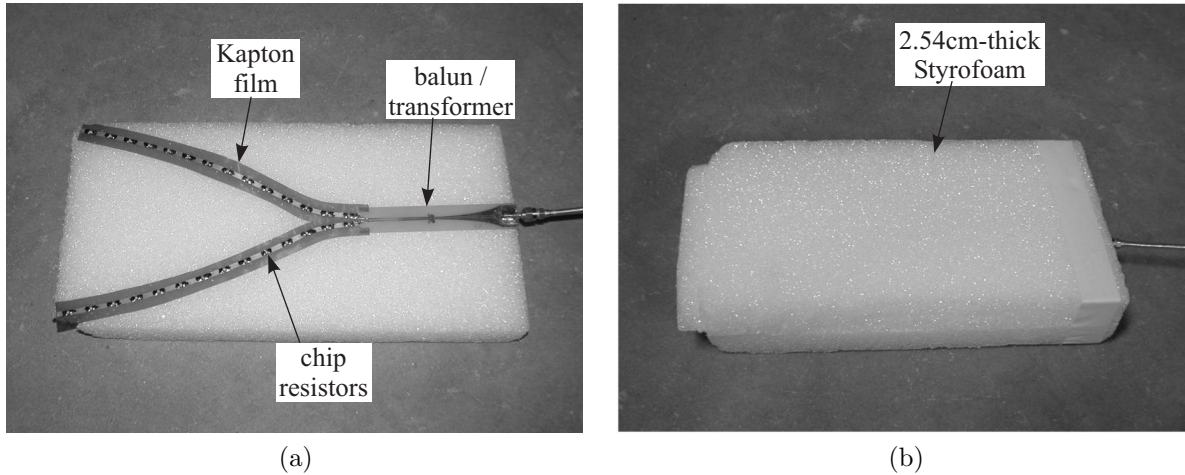


Figure 8. Photographs of the RLA: (a) antenna and balun on a polystyrene foam block; and (b) antenna and balun squeezed between two blocks of polystyrene foam.

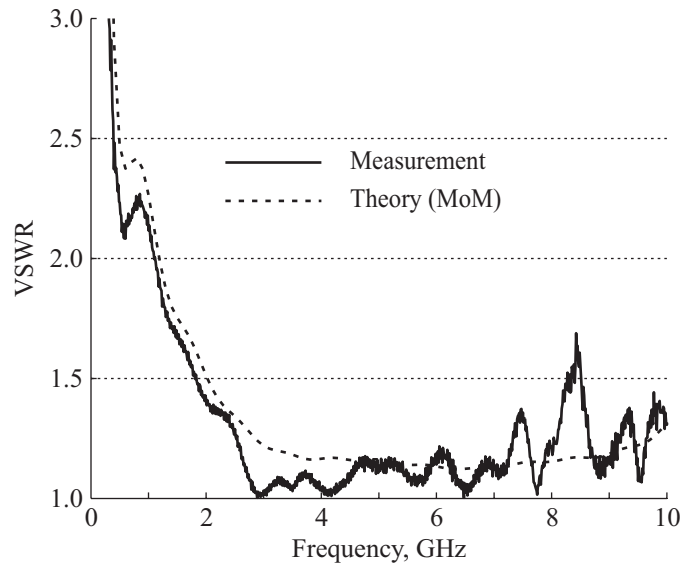


Figure 9. Comparison of the measured VSWR and numerical VSWR of the manufactured antenna when it is connected to a 188Ω feed line.

Because the gain is identical for both antennas, it can be obtained by inverting the following equation at each frequency:

$$|S_{21}|^2 = G_0(f)^2 \left(\frac{\lambda}{4\pi R} \right)^2, \quad (6)$$

where $G_0(f)$ is the gain of the antenna at a frequency, and λ is the wavelength at the frequency.¹⁴ The figure shows that the antenna module performs well at low frequencies. Its performance is degraded at high frequencies because of the loss in the balun.

The use of the RLA in a GPR is demonstrated by forming a bistatic radar using the two antennas separated by 11.43cm and pointing them toward the same direction. Four landmines, i.e., VS-1.6, VS-50, TS-50, and VS-2.2, are used as buried targets, which are buried along the y -direction at depths 6cm, 1cm, 1cm, and 6cm from the surface, respectively. The GPR is scanned approximately 2cm high above the ground (Fig. 11). The response is obtained as functions of y -coordinate and frequency. The y and frequency grids consist of 91 points

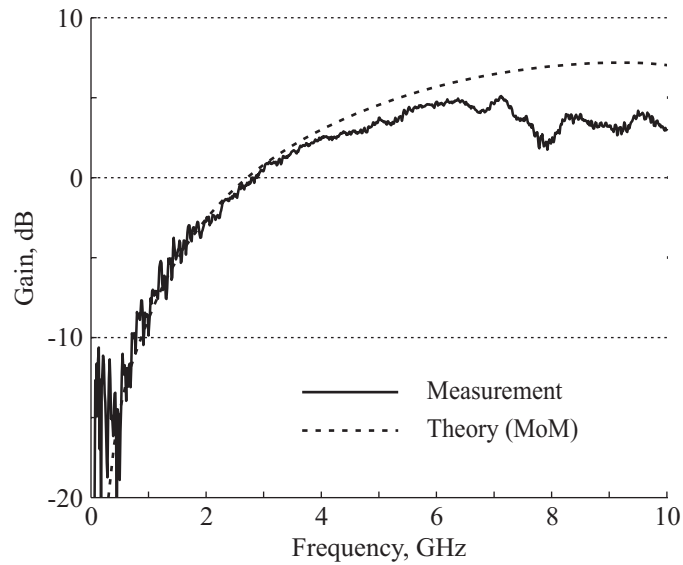


Figure 10. Comparison of the measured and numerical gains of the manufactured antenna. In the numerical model, the antenna is fed by a 200Ω balanced transmission line, and the gain is measured at the drive point. In the measurement, the antenna is fed by the double-Y balun, and the gain is measured at the balun input port.

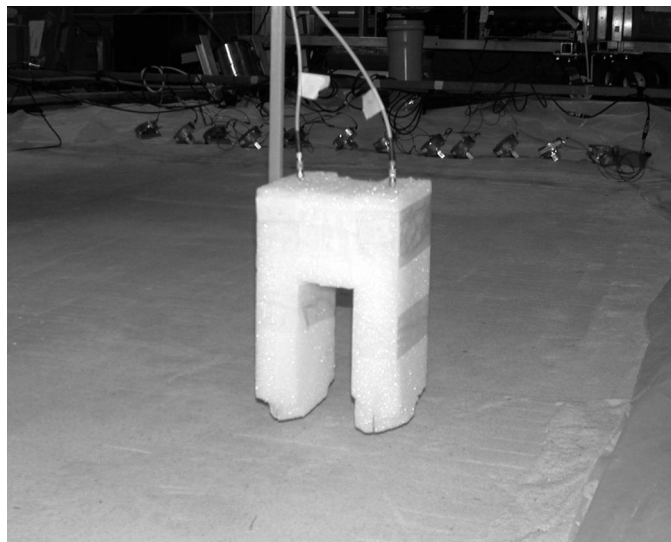


Figure 11. Photograph of the two identical RLA's forming a GPR. The two antennas are separated by 11.43cm and fixed to a plastic rod, which is connected to a position controller.

with 2cm increment and 401 points from 500MHz to 8.5GHz with 20MHz increment, respectively. The frequency response is then transformed to the time domain for a differentiated Gaussian pulse incident in the feed line with the center frequency of 2.5GHz.

The experiment was performed at the Electromagnetics/Acoustics Laboratory at the Georgia Institute of Technology. Fig. 12 shows the results in a pseudo-color image, which plots the received voltage in the space-time domain. The horizontal axis represents the y-coordinate, and the vertical axis represents the time. The big horizontal response centered at 1.6nsec is the return from the surface of the ground. The landmines are clearly seen later in time. The first reflections from the 1cm-deep targets are seen around 1.8nsec, and the first reflections from the 6cm-deep targets are seen around 2.75nsec. The speed of wave propagation in the test soil is roughly a third of the speed of light in free space. For large targets such as VS-1.5 and VS-2.2, the reflections from the

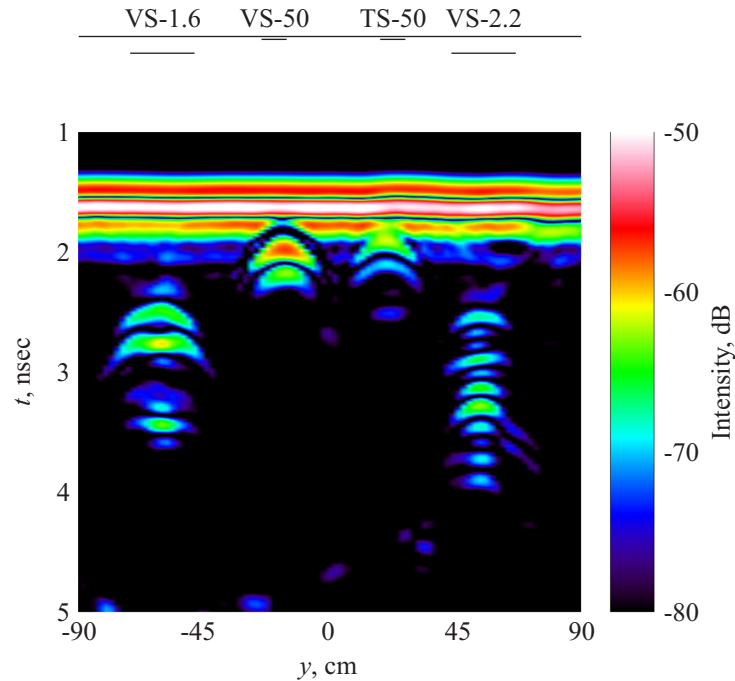


Figure 12. GPR scan result of the landmines in a pseudo-color graph. The graph shows the signal intensities in a 30-dB scale. The vertical axis represent the time, and the horizontal axis represent the position of the GPR. The lines above the pseudo-color graph show the relative sizes and depths of the landmines schematically.

top and bottom of the target are distinguishable.

5. CONCLUSION

The RVD was improved and referred to as RLA in this work. The RLA was shown to perform better than the RVD in terms of VSWR, gain, and F/B. The RLA was comparable to the RVD in terms of RCS. The improvement was achieved by using curved arms loaded with a modified Wu-King profile instead of straight arms loaded with the Wu-King profile.

The designed antenna was manufactured by printing the arms on a thin Kapton film and loading them with chip resistors. The antenna arms and the balun were squeezed between two polystyrene foam blocks to enhance the mechanical strength and to protect the delicate components. The performance of the manufactured antenna was validated by measurements. The use of the RLA in a bistatic GPR was also demonstrated.

ACKNOWLEDGMENTS

This work is supported in part by the US Army Night Vision and Electronic Sensors Directorate, Science and Technology Division, Countermines Branch and in part by the U. S. Army Research Office under Contract Number DAAD19-02-1-0252.

REFERENCES

1. T. P. Montoya and G. S. Smith, "Resistively-loaded vee antennas for short-pulse ground penetrating radar," in *IEEE Int. Antennas Propagat. Symp. Dig.*, pp. 2068–2071, Jul. 1996.
2. T. P. Montoya, *Vee Dipole Antennas for Use in Short-Pulse Ground-Penetrating Radars*. PhD thesis, Georgia Institute of Technology, Mar. 1998.
3. Kangwook Kim, *Numerical and Experimental Investigation of Impulse-Radiating Antennas for Use in Sensing Applications*. PhD thesis, Georgia Institute of Technology, April 2003.

4. T. T. Wu and R. W. P. King, "The cylindrical antenna with nonreflecting resistive loading," *IEEE Trans. Antennas Propagat.* **AP-13**(3), pp. 369–373, May 1965. Correction: L. C. Shen and R. W. P. King, vol. 13, no. 6, p. 998, Nov. 1965.
5. J. G. Maloney and G. S. Smith, "A study of transient radiation from the Wu-King resistive monopole - FDTD analysis and experimental measurements," *IEEE Trans. Antennas Propagat.* **41**(5), pp. 668–676, May 1993. Correction: J. G. Maloney and G. S. Smith, vol. 43, no. 2, p. 226, Feb. 1995.
6. T. P. Montoya and G. S. Smith, "Vee dipoles with resistive loading for short-pulse ground-penetrating radar," *Microwave Optical Tech. Lett.* **13**(3), pp. 132–137, Oct. 1996.
7. T. P. Montoya and G. S. Smith, "Land mine detection using a ground-penetrating radar based on resistively loaded vee dipoles," *IEEE Trans. Antennas Propagat.* **47**(12), pp. 1795–1806, Dec. 1999.
8. Kangwook Kim and W. R. Scott, Jr., "Design and realization of a discretely loaded resistive vee dipole for ground-penetrating radars." accepted by *Radio Science* for publication in the special section *Sensing of Landmines: Modeling, Measurements and Signal Processing*.
9. Kangwook Kim and W. R. Scott, Jr., "Design and realization of a discretely loaded resistive vee dipole on a printed circuit board," in *Detection and Remediation Technologies for Mines and Minelike Targets VIII, Proc. SPIE*, **5089**, pp. 818–829, April 2003.
10. K. C. Gupta, R. Garg, I. Bahl, and P. Bhartia, *Microstrip Lines and Slotlines*, Artech House, 2 ed., 1996.
11. R. M. Sharpe, J. B. Grant, N. J. Champagne, W. A. Johnson, R. E. Jorgenson, D. R. Wilton, W. J. Brown, and J. W. Rockway, "EIGER: Electromagnetic interactions generalized," in *IEEE AP-S Int'l Symp. Digest, Quebec, Canada*, pp. 2366–2369, Jul. 1997.
12. M. Kanda, "A relatively short cylindrical broadband antenna with tapered resistive loading for picosecond pulse measurements," *IEEE Trans. Antennas Propagat.* **26**(3), pp. 439–447, May 1978.
13. J. B. Venkatesan and W. R. Scott, Jr., "Investigation of the double-Y balun for feeding pulsed antennas," in *Detection and Remediation Technologies for Mines and Minelike Targets VIII, Proc. SPIE*, **5089**, pp. 830–840, April 2003.
14. C. A. Balanis, *Antenna Theory*, New York: John Wiley & Sons, Inc., 1982.